Pergamon

Bioorganic & Medicinal Chemistry 8 (2000) 2229–2241

BIOORGANIC & MEDICINAL CHEMISTRY

Template-Constrained Cyclic Peptide Analogues of Somatostatin: Subtype-Selective Binding to Somatostatin Receptors and Antiangiogenic Activity

Daniel J. Suich,[a,*,†] Shaker A. Mousa,[b] Gurke Singh,[c] George Liapakis,[c] Terry Reisine[c] and William F. DeGrado[a,*]

[a]*Department of Biochemistry and Biophysics, University of Pennsylvania, Philadelphia, PA 19104-6059, USA*
[b]*DuPont Pharmaceuticals Company, Wilmington, DE 19880, USA*
[c]*Department of Pharmacology, University of Pennsylvania, Philadelphia, PA 19104, USA*

Received 12 October 1999; accepted 4 May 2000

Abstract—β-Turns are a common secondary structure motif found in proteins that play a role in protein folding and stability and participate in molecular recognition interactions. Somatostatin, a peptide hormone possessing a variety of therapeutically-interesting biological acitivities, contains a β-turn in its bioactive conformation. The β-turn and biological activities of somatostatin have been succesfully mimicked in cyclic hexapeptide analogues. Two novel, structured, non-peptidic molecules were developed that are capable of holding the bioactive tetrapeptide sequence of somatostatin analogues in a β-turn conformation, as measured by somatostatin receptor (SSTR) binding. Template-constrained cyclic peptides in which the ends of the -Tyr-D-Trp-Lys-Val-tetrapeptide were linked by scaffolds based on either an *N,N′*-dimethyl-*N,N′*-diphenylurea or a substituted biphenyl system (**DJS631** and **DJS811**, respectively), bound selectively to mouse SSTR2B and rat and human SSTR5 with affinities as high as 1 nM. **DJS811**, at a dose of 3 mg/kg/day, was shown in a mouse Matrigel model to inhibit angiogenesis to a level of 79%. The development of structured turn scaffolds allows β-turn sequences to be contained in the context of a compact structure, with less peptidic nature and potentially greater bioavailability than cyclic hexapeptides. These systems can be used to study the determinants of β-turn formation, as well as to probe the importance of turn sequences occurring in molecular recognition interactions. The antiangiogenic activity of **DJS811** suggests that it may have antitumor activity as well. In addition, because SSTR2 is overexpressed on many types of tumors, **DJS631** and **DJS811** may be useful in the development of agents for tumor imaging or the radiotherapy of cancer.

Introduction

The β-turn is a common structural element in proteins which not only contributes to protein folding and stability, but also plays an important role in molecular recognition interactions.[1] Molecular interactions in which β-turns have been implicated as recognition elements include the binding of peptide hormones to their receptors,[1–3] antibody-antigen recognition,[4–7] post-translational modification of proteins,[1,8] and protein–protein interactions.[9–18] A means to contain the essential components of the β-turn structure in the context of a small molecule would be useful not only as a test bed to explore the requirements for turn formation, but also directly as a therapeutic agent or as a probe of the biological processes mediated by its binding interactions. Cyclic hexapeptides have been used for these purposes, as they contain two fused β-turn structures, in which the *i* residue of each turn corresponds to the *i*+3 residue of the other. While the cyclic nature of these structures gives them greater rigidity and hydrolytic stability than their linear analogues, these compounds can still suffer, due to their peptidic nature, from limited bioavailablity.

One way to decrease the peptide content of a cyclic hexapeptide while further increasing its conformational rigidity is to replace one of the β-turns with a synthetic compound, which can either mimic the bioactive turn itself, or serve as a structurally-constrained template or scaffold to present the remaining peptide in a β-turn conformation. A number of different compounds have been suggested as potential linkers for fixing the conformation

*Corresponding authors. Tel.: +1-215-898-4590; fax: +1-215-573-7229; e-mail: wdegrado@mail.med.upenn.edu
†Current address: Chiron Corporation, 4560 Horton St., Emeryville, CA 94608, USA.

0968-0896/00/$ - see front matter
PII: S0968-0896(00)00135-8

of cyclic peptides.[19,20] Such linkers include derivatives of 6-aminocaproic acids[21] (vide infra), napthalene derivatives,[22,23] *N*-methyl-β-lactam derivatives,[24] and α-benzyl-*o*-aminomethylphenylacetic acid derivatives.[25] β-Amino acids have also been used as templates for incorporation into cyclic peptides.[26,27] Kelly and co-workers have similarly made use of dibenzofurans and biaryl-based amino acids to encourage turn formation.[19] A diphenylacetylene derivative has also been shown to substitute well for a turn-forming dipeptide in β-hairpins.[28] Nagai's bicyclic dipeptide turn mimetic BTD has been incorporated into a number of different bioactive peptides and proteins,[12,29,30] and benzodiazepine derivatives have been incorporated into the cyclic peptide gramicidin S with retention of activity.[31] Finally, the simple *trans*-dipeptide mimetic, *m*-aminomethylbenzoic acid (mamb), has been independently developed by von Itzstein[32] and our own group[33] to stabilize turn conformations in cyclic peptides. In the present work, we have sought to extend this approach by developing structurally-constrained scaffolds capable of presenting a tetrapeptide sequence such that the two central residues adopt a turn conformation without any additional backbone constraints. A structure of this type would provide a general system to study the parameters affecting β-turn formation, as well as to generate bioactive mimetics of β-turns with potentially greater bioavailability and conformational rigidity than cyclic hexapeptides.

A simple means of determining the ability of a synthetic scaffold to accomodate a tetrapeptide in the desired β-turn conformation is to employ a bioactive peptide sequence which requires such a conformation for high-affinity receptor binding. The ability of the constrained peptide to bind to the receptor is then a direct measure of how well the tetrapeptide adopts the required turn conformation. For this purpose, we chose to mimic the cyclic peptide hormone somatostatin (Table 1),[34] for which the bioactive conformation is known to be a β-turn,[35] and for which five receptor subtypes have been cloned and expressed.[36] A potent cyclic hexapeptide analogue of somatostatin, MK-678 (Table 1), contains the sequence -Tyr-D-Trp-Lys-Val-, of which the central -D-Trp-Lys- dipeptide forms the $i+1$ and $i+2$ residues of a βII′-turn necessary for high affinity receptor binding.[37] Mimicry of somatostatin thus provides a simple means of detecting the adoption of the desired turn conformation. Additionally, the development of somatostatin analogues is desirable due to the diverse, therapeutically-relevant biological activities of the natural hormone. Somatostatin not only inhibits exocrine secretions and the release of endocrine hormones such as growth hormone, insulin, glucagon, and gastrin, but also acts as a neurotransmitter and has direct anti-proliferative effects on cells[36] (vide infra). Somatostatin analogue agonists have been used therapeutically for the control of acromegaly and certain endocrine tumors, and as tumor imaging agents.[36,38] While diabetes has been treated with somatostatin agonists because of their ability to inhibit growth hormone release, antagonists of SSTR5, capable of blocking the inhibition of insulin release from the pancreas, would also be useful in the treatment of type II diabetes.[36,39,40] Somatostatin analogues such as MK-678 (seglitide) and the cyclic octapeptides Sandostatin (octreotide, SMS 201-955) and RC-160 (Table 1), all agonists, have been shown to inhibit angiogenesis, the process by which new blood vessels are formed.[41,42] There has been substantial recent interest in the inhibition of angiogenesis as a means of inhibiting tumor growth and metastasis, as well as in the treatment of diseases such as diabetic retinopathy and rheumatoid arthritis.[41–43] The interest in and therapeutic potential of somatostatin analogues is underscored by efforts to generate libraries of somatostatin mimetics,[44] and the recent development of selective, non-peptide agonists of somatostatin receptors.[45–48]

Table 1. Structures of somatostatin and analogues

Somatostatin-14	Ala-Gly-c[Cys-Lys-Asn-Phe-Phe-Trp-Lys-Thr-Phe-Thr-Ser-Cys]-OH
MK-678	c[N-Me-Ala-Tyr-D-Trp-Lys-Val-Thr]
Sandostatin	D-Phe-c[Cys-Phe-D-Trp-Lys-Thr-Cys]-Thr-ol
RC-160	D-Phe-c[Cys-Tyr-D-Trp-Lys-Val-Cys]-Thr-NH_2

In this paper, we describe the design and synthesis of two novel synthetic scaffolds capable of presenting a tetrapeptide sequence in a β-turn conformation. Cyclic peptide compounds in which these templates were used to display the -Tyr-D-Trp-Lys-Val- tetrapeptide turn sequence from MK-678 bound to cloned somatostatin receptors in vitro with high affinity and selectivity. The more potent of the analogues was further analyzed for its ability to inhibit angiogenesis in a mouse model, and exhibited strong antiangiogenic activity.

Results and Discussion

Design of turn scaffolds

The first role that a turn scaffold molecule must fulfill is that of geometry. Not only does the structure need to be capable of joining the two ends of a tetrapeptide, it must also bridge the gap in such a way as to allow the peptide to adopt a turn conformation. A second requirement is that the molecule itself contains significant conformational constraint, such that it can hold the ends of the tetrapeptide in the appropriate orientation without significantly changing its own conformation. Two molecules that could simultaneously fulfill both of these requirements are shown in Figure 1. In Figure 1A is depicted an *N,N′*-diphenylurea, which by virtue of its *N,N′*-dimethyl substitution is expected to adopt a cisoid geometry wherein the two aromatic rings lie adjacent and parallel to each other, based on the X-ray structural analysis of related compounds by Shudo and co-workers.[49] The plane of the rings is expected to be perpendicular to that of the urea moiety (***a***). Given such a conformation, the attached amide groups should then be adjacent to each other as shown, at a distance capable of bridging the ends of a tetrapeptide in a β-turn conformation. Because the amides are directly attached to the aromatic system, rotation about bonds ***b*** and ***c*** is expected to be constrained to dihedral angles of $\pm 25^\circ$ between the plane of the amide and that of the aromatic ring. These

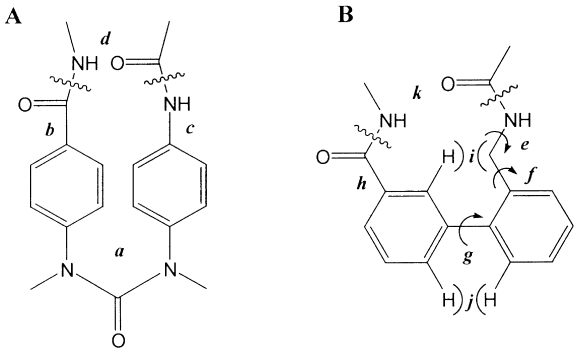

Figure 1. Parameters affecting conformational flexibility and constraint in designed β-turn scaffolds. Panel A depicts an *N*,*N*′-dimethyl-*N*,*N*′-diphenylurea system in which constraint is conferred by the cisoid geometry of the substituted urea **a**, restricted rotation about bonds **b** and **c**, and hydrogen bond **d**. Panel B depicts a substituted biphenyl system in which flexibility is provided by free rotation about bonds **e**, **f**, and **g**, and constraint is imposed by restricted rotation about bond **h**, steric clashes **i** and **j** between substituents *ortho* to the interaromatic bond, and hydrogen bond **k**.

values for the dihedral angle were observed in a search of relevant small-molecule crystal structures in the Cambridge database, and can be explained by the balance of two opposing forces. Coplanarity is favored due to overlap between the π systems of the amide and aromatic ring, but disfavored due to steric clashes between the amide and hydrogens *ortho* to the point of attachment. Finally, this structure should allow the first and last amide of an attached peptide to hydrogen bond to each other as indicated by ***d***. Such a hydrogen bond corresponds to that between residues *i* and *i*+3 of a cyclic hexapeptide, and its presence would provide further conformational constraint on the system.

The biphenyl compound shown in Figure 1B was also anticipated to fulfill the requirements of appropriate geometry and conformational constraint necessary for a turn scaffold. The conformational space available to this structure is limited by the restricted rotation about the interaromatic single bond ***g*** due to a balance of opposing effects. Overlap of the π systems of the rings favors their coplanarity, whereas steric clashes between substituents *ortho* to the interaromatic linkage such as hydrogen atoms and the methylamino group (***i*** and ***j***) disfavor coplanarity. For the same reasons discussed above for the substituted urea system, the direct attachment of the carboxyl group to the biphenyl moiety (***h***) provides further constraint, with an expected dihedral angle of ±25°. Again, as for the substituted urea system, the conformation of the biphenyl system should allow hydrogen bonding to occur between the first and last amides of an attached peptide, providing additional constraint. At the same time, flexibility is present in this structure that should allow the molecule to adopt a conformation capable of connecting the ends of a tetrapeptide in a β-turn conformation. Flexible connections are provided by the two rotatable single bonds in the methylamino substiuent (***e*** and ***f***), as well as the soft potential asssociated with the interaromatic single bond (***g***).

The ability of each of these scaffold structures to connect the ends of a tetrapeptide adopting the βII′ turn conformation found in cyclic hexapeptide analogues of somatostatin while still adopting a favorable conformation themselves was assessed and confirmed by molecular modeling. Structures were built in which each scaffold was linked to the ends of the tetrapeptide -Ala-D-Ala-Ala-Ala-. This tetrapeptide was used in lieu of the actual peptide sequence of somatostatin analogues in order to make the modeling less computationally intensive, while still providing the constraint conferred by α substituents in the peptide chain. When the ϕ and ψ angles of the central -D-Ala-Ala- dipeptide of the structures were restrained to those of a canonical βII′ turn (60°, −120°, −80°, 0°) and the structures were energy minimized, reasonable conformations were obtained for the scaffold moieties, in accordance with the considerations discussed above (Figs 2 and 3). Analysis of these structures by

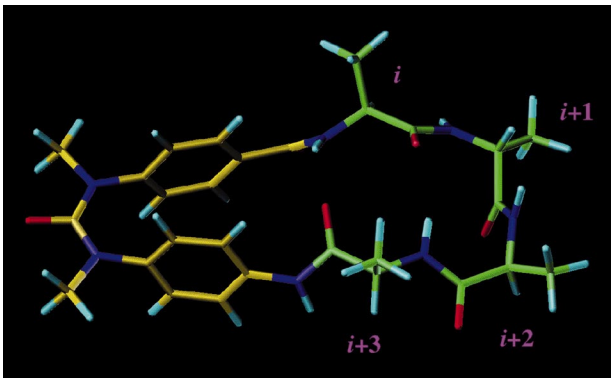

Figure 2. Energy-minimized model of template-constrained cyclic peptide in which the *N*,*N*′-dimethyl-*N*,*N*′-diphenylurea scaffold links the ends of the tetrapeptide -Ala-D-Ala-Ala-Ala-. The ϕ and ψ angles of the *i*+1 (D-Ala) and *i*+2 residues of the peptide have been constrained to those of a canonical βII′-turn. The carbon atoms of each scaffold are in yellow, and those of the peptides are in green; oxygens atoms are red, nitrogens blue, and hydrogens cyan.

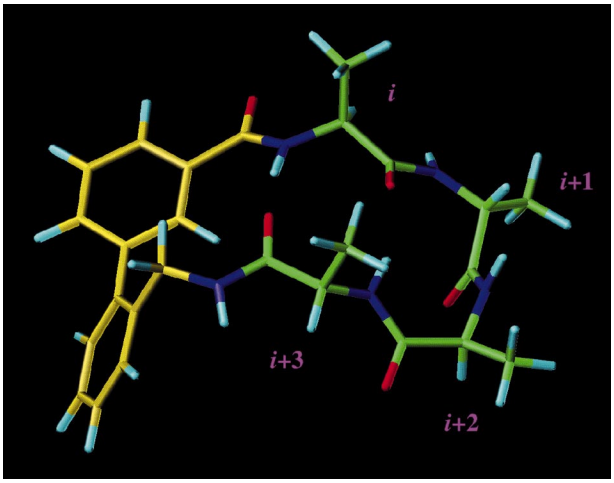

Figure 3. Energy-minimized model of template-constrained cyclic peptide in which the substituted biphenyl scaffold links the ends of the tetrapeptide -Ala-D-Ala-Ala-Ala-. The ϕ and ψ angles of the *i*+1 (D-Ala) and *i*+2 residues of the peptide have been constrained to those of a canonical βII′-turn. The carbon atoms of each scaffold are in yellow, and those of the peptides are in green; oxygens atoms are red, nitrogens blue, and hydrogens cyan.

dynamics and energy minimization without any restraints on the peptide conformation revealed that while the substituted urea system is fairly rigid, the biphenyl system confers significant flexibility on the structure, an observation that is congruent with the presence of rotatable bonds in the biphenyl system as noted in the discussion above.

Synthesis of cyclic peptide analogues of somatostatin incorporating turn scaffolds

The cyclic peptide analogues of somatostatin incorporating the urea and biphenyl turn scaffolds discussed above were synthesized as laid out in Schemes 1, 2, and 3.

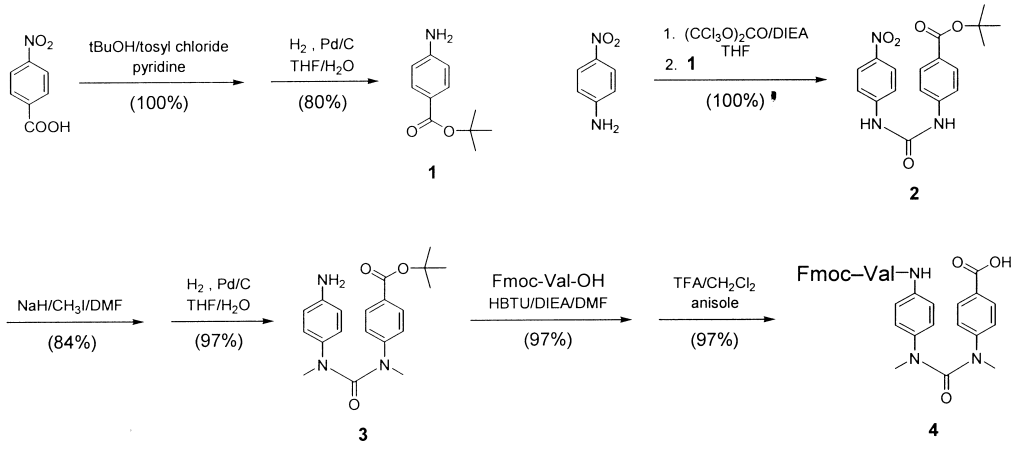

Scheme 1. Synthesis of the *N*,*N*′-dimethyl-*N*,*N*′-diphenylurea scaffold derivatized with FmocVal.

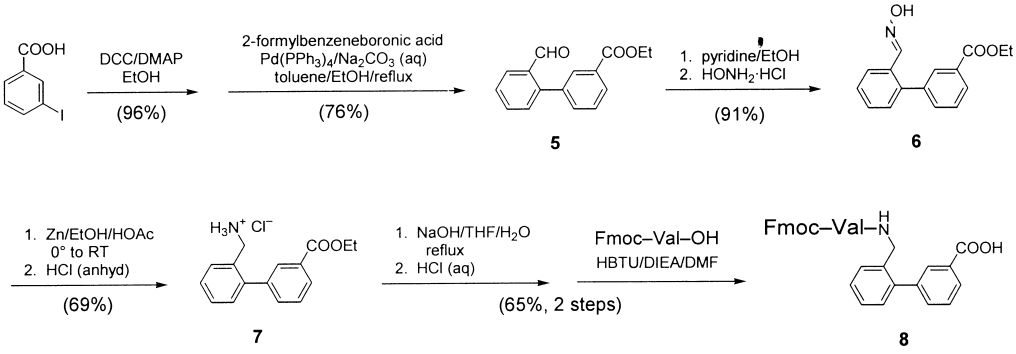

Scheme 2. Synthesis of the substituted biphenyl scaffold derivatized with Fmoc-Val.

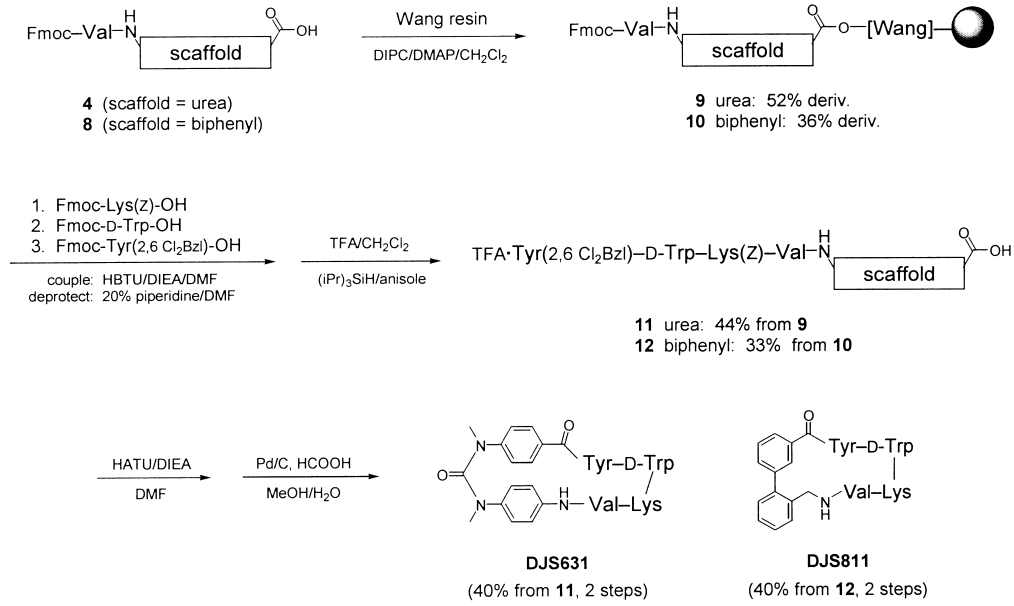

Scheme 3. Incorporation of Fmoc-Val-derivatized β-turn scaffolds into template-constrained cyclic peptide somatostatin analogues **DJS631** and **DJS811**.

In each case, the scaffold was synthesized in solution, followed by coupling of Fmoc-L-valine (Fmoc = 9-fluorenylmethyloxycarbonyl), corresponding to the last residue of the tetrapeptide, using standard solution phase methods. Next, these intermediates were extended using solid-phase peptide synthesis methods to introduce the remainder of the tetrapeptide sequence. After cleavage of the linear, protected intermediates containing the scaffolds from the resin, cyclization and deprotection in solution afforded the desired products.

For the urea scaffold, the *t*-butyl ester of 4-aminobenzoic acid **1** was coupled to 4-nitroaniline with triphosgene to afford the unsymmetrical urea intermediate **2**. Methylation of **2** with CH_3I, followed by catalytic reduction of the nitro group afforded the *t*-butyl ester-protected aniline derivative **3**. After coupling of Fmoc-L-Val-OH to **3** using 2-(1*H*-benzotriazol-1-yl)-1,1,3,3-tetramethyluronium hexafluorophosphate (HBTU), the *t*-butyl ester was cleaved to afford the Fmoc-valine-derivatized urea scaffold as the free acid (**4**) in 61% overall yield. The synthesis of the Fmoc-valine-derivatized biphenyl scaffold begins with the coupling of ethyl 3-iodobenzoate to the commercially-available 2-formylbenzeneboronic acid under Suzuki conditions to generate the biphenyl nucleus **5**. Oxime formation using hydroxylamine hydrochloride, followed by reduction with Zn^0 afforded the desired 2-aminomethyl derivative **7** isolated as the hydrochloride salt. The zwitterion resulting from saponification of the ethyl ester in **7** was coupled with Fmoc-L-Val-OH using HBTU to yield the Fmoc-valine-derivatized biphenyl scaffold as the free acid (**8**) in 30% overall yield.

Each of the Fmoc-valine-derivatized scaffold free acids **4** and **8** were coupled to Wang resin using diisopropylcarbodiimide (DIPC) and 4-(dimethylamino)pyridine (DMAP) in CH_2Cl_2. Using standard Fmoc peptide synthesis methodology, Fmoc-L-Lys(Z)-OH (Z = benzyloxycarbonyl), Fmoc-D-Trp-OH, and Fmoc-L-Tyr(2,6-dichlorobenzyl)-OH were coupled in succession to the resin-bound intermediates using HBTU. Cleavage of the linear intermediates from the resin with a cocktail containing trifluoroacetic acid (TFA) and cation scavengers in CH_2Cl_2 afforded side-chain-protected peptides **9** and **10** which incorporate the turn scaffolds at their C-termini. These intermediates were cyclized in solution using 2-(7-aza-1*H*-benzotriazol-1-yl)-1,1,3,3-tetramethyluronium hexafluorophosphate (HATU) at a peptide concentration of 10 mM, and the protecting groups were removed from the side chains via catalytic reduction to afford the desired template-constrained cyclic peptide somatostatin analogues **DJS631** and **DJS811** as their TFA salts after purification by reverse-phase high pressure liquid chromatography (HPLC).

Binding of cloned somatostatin receptors (SSTRs) by DJS631 and DJS811

As shown in Table 2, compounds **DJS631** and **DJS811** bound selectively to somatostatin receptors SSTR2B (mouse, m) and SSTR5 (rat, r and human, h). In each case, the compounds bound more tightly to SSTR2B and with lower affinity to SSTR5, and **DJS811** bound to the receptors more tightly than **DJS631**. The IC_{50}s of **DJS631** and **DJS811** for mSSTR2B, 7 and 1.0 nM, respectively, compare favorably with that of somatostatin for this receptor, 0.6 nM (Table 2).[50] Both compounds have a similar preference for binding mSSTR2B over rSSTR5, with **DJS631** binding 11-fold more potently to mSSTR2B, and **DJS811** with a 13-fold preference for this receptor. **DJS631** discriminates between rat and human SSTR5 (IC_{50}s of 80 and 220 nM, respectively) to a greater extent than does **DJS811** (IC_{50}s of 13 and 15 nM, respectively). **DJS811** is more similar to somatostatin in this regard, which has nearly equal affinity for these two receptors (0.3 and 0.2 nM, respectively).[36] The pattern of selectivity of **DJS631** and **DJS811** for the cloned somatostatin receptors, in that they have high affinity for SSTR2 and SSTR5, but do not bind to the others, is similar to that of analogues such as MK-678 and Sandostatin, except that these latter analogues do have limited affinity for SSTR3 (Table 2).[36] Somatostatin, by contrast, binds to all receptor subtypes with similar affinity, in the tenth-nanomolar to nanomolar range.[36]

The higher affinity of **DJS811** overall for the somatostatin receptors compared with **DJS631** could be attributed to either of two factors. One is the greater hydrophobicity of **DJS811**, a property inferred from its greater retention time by reverse-phase HPLC. A second is the apparent greater flexibility of **DJS811** compared with **DJS631** seen in the molecular modeling studies discussed previously. In the first case, a more hydrophobic ligand would be expected to bind with higher affinity to a lipophilic receptor than a more polar ligand, due to the hydrophobic effect. A correlation between greater

Table 2. Affinities of **DJS631** and **DJS811** for cloned somatostatin receptors[a]

	IC_{50} (nM)				
Receptor	**DJS631**	**DJS811**	Somatostatin	MK-678	Sandostatin
hSSTR1	> 1000 (2)	> 1000 (2)	0.1	> 1000	> 1000
mSSTR2B	7 (3)	1.0 (3)	0.6	0.1	0.2
mSSTR3	~1000 (2)	> 1000 (2)	0.1	268	150
hSSTR4	> 1000 (1)	ND	1.2	> 1000	> 1000
rSSTR5	80 (3)	13 (3)	0.3	1.3	0.2
hSSTR5	220 (3)	15 (3)	0.2	23	32

[a]Results of radioligand displacement assay for **DJS631** and **DJS811** against cloned human (h), mouse (m), and rat (r) somatostatin receptors (SSTRs). IC_{50} values calculated (in nM) represent the concentration of **DJS631** or **DJS811** capable of displacing half of the bound radioligand [^{125}I]tyr^{11}-somatostatin-14 from the receptor in vitro. The number of experiments is indicated in parentheses. Affinities of somatostatin, MK-678, and Sandostatin for these receptors measured by a similar method are shown for comparison.[36,50]

hydrophobicity and higher potency for cyclic hexapeptide somatostatin analogues has been observed.[37] In the second case, one would generally argue that flexibility in a ligand would decrease its affinity for a receptor, compared with a ligand that is rigidly held in an optimal binding conformation, due to the greater amount of entropy loss upon binding for the more flexible molecule. However, if the more rigid ligand is locked in a suboptimal binding conformation, a similar but more flexible ligand may be able to offset the negative effect of entropy losses upon binding by having access to a conformation optimal for receptor interaction, and as a result bind more tightly than the rigid ligand. By either line of reasoning, **DJS811**, being both more hydrophobic and putatively more flexible than **DJS631**, would be expected to bind with higher affinity overall to the receptors, which could explain the affinities observed in Table 2. The greater flexibility of **DJS811** can also explain the lower discrimination **DJS811** displays in binding rat versus human SSTR5 than does **DJS631**. A flexible ligand has a greater ability than a more rigid one to adjust to subtle differences in the binding sites of various receptor subtypes, and bind to them despite those differences.

Antiangiogenic activity of DJS811

Using a mouse model in which capillary growth is induced in an implanted gel matrix called Matrigel,[51] the ability of **DJS811** to inhibit angiogenesis was tested. A positive control, in which mice (eight animals) were subcutaneously injected with Matrigel containing basic fibroblast growth factor (bFGF) gave a value of 2.9±0.4 g/dL hemoglobin content after a period of 7 days (Table 3). For similarly-treated mice (10 animals) that in addition received an infusion of 3 mg/kg/day of **DJS811**, hemoglobin content of the Matrigel after the same time period was only 0.68±0.41 g/dL, which represents a 79±18% inhibition of angiogenesis. The negative control group, which received Matrigel implants, but no bFGF and no **DJS811** (10 animals) gave a hemoglobin content of 0.08±.01 g/dL. Importantly, every mouse treated with **DJS811** showed a significant response to the treatment. Visualization of gel slices stained by an immunohistochemical method sensitive to the presence of platelet endothelial cell adhesion molecule-1 (PECAM-1) protein found in blood vessels confirmed the inhibition of capillary growth in mice treated with **DJS811**.

Table 3. Antiangiogenic activity of **DJS811** in the mouse Matrigel model[a]

	Positive control	Treated
	3.3	0.81
	2.8	0.16
	2.6	0.04
	3.7	0.38
	3.0	0.56
	3.0	0.63
	2.5	1.05
	2.4	0.78
		1.27
		1.16
Mean±SD	2.9±0.4	0.68±0.41
	Inhibition level: 79±18%	

[a]Values for hemoglobin content, reported in g/dL, of bFGF-treated Matrigel implanted in mice for 7 days. Each listed value is from an individual animal. The treated group received 3 mg/kg/day of **DJS811**, while the positive control group did not. A 79% level of inhibition of angiogenesis was calculated from these data as described in the text.

Given the receptor subtype selectivity of **DJS811**, there are at least two possible explanations as to its mode of action in inhibiting new blood vessel formation. One possibility is the inhibition of growth hormone release, as has been suggested for the observed antiangiogenic effect of Sandostatin and RC-160 in the chicken chorioallantoic membrane model,[42] as well as the inhibition of retinal neovascularization by MK-678.[41] High affinity agonist binding to SSTR2 has been shown to mediate the inhibition of growth hormone release.[36,52] Given its high affinity for SSTR2, **DJS811** may also inhibit angiogenesis by this mechanism. Another mechanism by which the antiangiogenic activity may be mediated is the stimulation of tyrosine phosphatase activity induced by binding of agonist analogues of somatostatin to SSTR2[53,54] or possibly SSTR5.[55,56] Stimulation of such tyrosine phosphatase activity by the binding of **DJS811** to SSTR2 or SSTR5 could counteract the effects of endothelial cell transmembrane receptor tyrosine kinases which mediate the angiogenic process.[57,58]

Conclusions

We have synthesized two novel structured scaffolds designed to present a tetrapeptide sequence in a turn conformation without additional backbone constraints. Scaffolds based on both *N,N′*-dimethyl-*N,N′*-diphenylurea and substituted biphenyl systems were designed using molecular modeling techniques, taking into consideration both conformational constraint and flexibility within these systems. The designed scaffold molecules were synthesized readily in good overall yield, and were then incorporated into cyclic peptides containing the bioactive tetrapeptide sequence from the somatostatin analogue MK-678. Both of these template-constrained cyclic peptides **DJS631** and **DJS811** bound selectively to cloned somatostatin receptors mSSTR2 and rat and human SSTR5 with high affinity, indicating that the tetrapeptide sequence was indeed adopting a β-turn conformation about the central -D-Trp-Lys- dipeptide as intended. The exact conformation of the tetrapeptide sequence and the scaffolds in these molecules is currently under further investigation by NMR. This work parallels that of van Binst and co-workers, who have demonstrated SSTR2-selective binding of both diastereomers of a template-constrained cyclic peptide containing a similar tetrapeptide sequence and racemic α-benzyl-*o*-aminomethylphenylacetic acid as a template.[25,59] The development of structured turn scaffolds allows turn sequences to be contained in the context of a compact structure. These molecules might display greater stability and bioavailability than their cyclic hexapeptide counterparts, and can be used to probe the importance of turn sequences occurring in molecular recognition interactions. Additionally, such systems can be used to study

the determinants of turn formation in proteins and peptides by varying the tetrapeptide that is incorporated. For example, the importance of the relative spatial orientation of the ends of the peptide, enforced by the scaffold, could be compared to the role of local interactions such as chirality and side chain–side chain interactions in determining the turn conformation.[21,60,61] We have also shown **DJS811** to be a potent inhibitor of angiogenesis in a mouse Matrigel model, suggesting that this compound may have antitumor activity as well; this possibility is currently under investigation. Finally, because somatostatin receptors, particularly SSTR2, are overexpressed on many types of tumor cells, both **DJS631** and **DJS811** may be useful in the development of agents for tumor imaging or radiotherapy of cancer.[62,63]

Experimental

Molecular modeling

The software packages Insight II 95.0/Discover 2.9.7 (Biosym/MSI) and Sybyl 6.03 (Tripos Associcates) were utilized in visualizing and energy minimizing structures. Sybyl was utilized for the dynamics and energy minimization studies, using the tripos force field, a temperature of 800 K, a dielectric constant of 15, and a 50 ps run time with snapshots taken every 50 fs for the dynamics runs. The 500 lowest energy structures were energy minimized and analyzed.

Synthesis of DJS631 and DJS811

General. The purity of peptide derivatives was assessed and the progress of reactions involving peptide derivatives was monitored using analytical reverse-phase HPLC on a C18 column, with mobile phases consisting of water and CH_3CN containing 0.1% TFA. Purified synthetic intermediates were characterized by ^1H NMR and high-resolution mass spectrometry (HRMS), and were judged to be pure by either thin-layer chromatography (silica gel) or reverse-phase HPLC, as appropriate.

***tert*-Butyl 4-nitrobenzoate.** To a slurry of 4-nitrobenzoic acid (16.71 g, 100 mmol) in 200 mL pyridine was added tosyl chloride (38.13 g, 200 mmol) with stirring. Once the solid was completely dissolved, the solution was chilled to 0 °C, and *tert*-butanol (7.41 g, 100 mmol) was added. After stirring at 0 °C for 2 h, the reaction mixture was allowed to warm to room temperature. After an additional 2 h of stirring, another portion of *tert*-butanol (7.41 g, 100 mmol) was added. The reaction mixture was allowed to stir for an additional 14 h. The solvent was evaporated, and the residue was partitioned between EtOAc and saturated $NaHCO_3$. The organic layer was washed three times with saturated $NaHCO_3$, and the pooled aqueous layers were washed once with EtOAc. The organic layers were pooled and washed once with brine, four times with 1 N $NaHSO_4$, once more with brine, and finally dried with $MgSO_4$. The solvent was evaporated to give the title compound (22.32 g, 100%) as a light-yellow solid. ^1H NMR ($CDCl_3$, 300 MHz) δ 8.26 (d, 2H, J = 9.0 Hz), 8.15 (d, 2H, J = 9.0 Hz), 1.62 (s, 9H). HRMS: calcd for $C_{11}H_{14}NO_4$ $(M+H)^+$, 224.0923; found, 224.0922.

***tert*-Butyl 4-aminobenzoate (1).** *tert*-Butyl 4-nitrobenzoate (22.32 g, 100 mmol) was dissolved in tetrahydrofuran (THF) (120 mL) and H_2O (40 mL), and Pd/C (10 wt% Pd, 1.064 g, 1 mol% Pd) was added. The reaction vessel was purged with Ar, then H_2, and pressurized with H_2 to 53 psi. The reaction mixture was allowed to shake at room temperature for 19 h. The reaction vessel was purged with Ar, the reaction mixture was filtered through Celite, and the filter bed was washed with CH_3CN. The filtrate was concentrated in vacuo, and to the resulting solid residue was added saturated $NaHCO_3$ and EtOAc. The pH of the mixture was adjusted to 10 with aqueous NaOH, the layers were shaken together and separated, and the aqueous layer was extracted three times more with EtOAc. The organic layers were combined, dried with $MgSO_4$, and the solvent was evaporated to afford **1** (15.41 g, 80%) as a light-orange crystalline solid. ^1H NMR (acetone-d_6, 300 MHz) δ 7.68 (d, 2H, J = 8.7 Hz), 6.64 (d, 2H, J = 8.7 Hz), 5.31 (br. s, 2H), 1.52 (s, 9H). HRMS: calcd for $C_{11}H_{15}NO_2$ $(M)^+$, 193.1103; found, 193.1098.

1-(4′-Nitrophenyl)-3-(4″-*tert*-butylcarboxyphenyl)urea (2). To 375 mL anhydrous THF under Ar was added 4-nitroaniline (12.24 g, 88.60 mmol) with stirring. After dissolution of the solid, the reaction mixture was cooled to 0 °C. Triphosgene (8.76 g, 29.5 mmol) was added, then diisopropylethylamine (DIEA) (30.87 mL, 177.2 mmol) was added in three portions over 5 min. The reaction mixture was allowed to stir for 5 min at 0 °C, then at room temperature for 45 min. The reaction mixture was again cooled to 0 °C. **1** (15.41 g, 79.74 mmol) was dissolved in 125 mL of anhydrous THF and added to the reaction mixture. The cooling bath was removed, and the reaction mixture was allowed to stir for an additional 42 h. The solvent was evaporated, and the residue was dissolved in CH_2Cl_2. The solution was extracted three times with 1 N $NaHSO_4$, at which point a solid began precipitating from the organic layer. The organic layer suspension was washed once with brine, and enough THF was added to the organic layer to bring the solid back into solution. The organic layer was dried with $MgSO_4$ and the solvent was evaporated. The residue was triturated with Et_2O, the mixture was filtered, and the solid was washed several times with Et_2O. The residual solvent was removed from the solid under vacuum to yield **2** (28.50 g, 100%) as a light-yellow solid. ^1H NMR (acetone-d_6, 300 MHz) δ 9.54 (s, 1H), 9.27 (s, 1H), 8.18 (d, 2H, J = 9.2 Hz), 7.88 (d, 2H, J = 8.8 Hz), 7.80 (d, 2H, J = 9.2 Hz), 7.65 (d, 2H, J = 8.8 Hz), 1.56 (s, 9H). HRMS: calcd for $C_{18}H_{19}N_3O_5$ $(M)^+$, 357.1325; found, 357.1335.

1-(4′-Nitrophenyl)-3-(4″-*tert*-butylcarboxyphenyl)-1,3-dimethylurea (2a). To 100 mL of anhydrous dimethylformamide (DMF) under Ar was added **2** (9.10 g, 25.5 mmol) with stirring. After dissolution of **2**, the reaction mixture was cooled to 0 °C in a bath, and NaH (60 wt%, 2.80 g, 70.0 mmol) was added in a single portion. After a further 5 min of stirring, CH_3I (17.4 mL, 280 mmol) was added, and the reaction mixture was allowed to stir at

0 °C for 15 min. The cooling bath was removed, and the reaction mixture was allowed to stir for 3 h at room temperature. The reaction was quenched by the addition of 1 N $NaHSO_4$ to a pH of 5. The solvent was evaporated in vacuo, and the residue was purified by silica gel flash column chromatography (eluted with 35% EtOAc in hexanes). The solvent was evaporated to yield **2a** (8.24 g, 84%) as a yellow solid. ^{1}H NMR (acetone-d_6, 300 MHz) δ 8.00 (d, 2H, J = 9.2 Hz), 7.74 (d, 2H, J = 8.8 Hz), 7.24 (d, 2H, J = 9.2 Hz), 7.16 (d, 2H, J = 8.7 Hz), 3.32 (s, 3H), 3.25 (s, 3H), 1.52 (s, 9H). HRMS: calcd for $C_{20}H_{24}N_3O_5$ $(M+H)^+$, 386.1716; found, 386.1717.

1-(4′-Aminophenyl)-3-(4″-*tert*-butylcarboxyphenyl)-1,3-dimethylurea (3). Compound **2a** (8.21 g, 21.3 mmol) was dissolved in 150 mL of THF and 50 mL of H_2O, and Pd/C (10 wt%, 227 mg, 1 mol% Pd) was added. The reaction vessel was purged with Ar, then H_2, and pressurized with H_2 to 55 psi. The reaction mixture was shaken at room temperature for 18 h, then the reaction vessel was purged with Ar, and the reaction mixture was filtered through Celite. The filter bed was washed with H_2O and THF. The filtrate was concentrated in vacuo, and the residue was partitioned between EtOAc and 1 N $NaHSO_4$. The organic layer was extracted nine more times with 1 N $NaHSO_4$, and 10 times with 1 N HCl. The aqueous layers were pooled and the pH was adjusted to 10.5 with the addition of aqueous NaOH. The aqueous solution was extracted four times with EtOAc, adjusting the pH up to 10.5 with aqueous NaOH after the first extraction. The organic layers were pooled, dried with $MgSO_4$, and the solvent was evaporated in vacuo to afford **3** (7.32 g, 97%) as a brown foam. ^{1}H NMR (acetone-d_6, 300 MHz) δ 7.72 (d, 2H, J = 8.9 Hz), 7.00 (d, 2H, J = 8.9 Hz), 6.69 (d, 2H, J = 8.8 Hz), 6.43 (d, 2H, J = 8.8 Hz), 4.54 (br. s, 2H), 3.12 (s, 3H), 3.05 (s, 3H), 1.54 (s, 9H). HRMS: calcd for $C_{20}H_{25}N_3O_3$ $(M)^+$, 355.1890; found, 355.1830.

1-(9‴-Fluorenylmethyloxycarbonyl-L-valyl-(4′-aminophenyl))-3-(4″-*tert*-butylcarboxyphenyl)-1,3-dimethylurea (3a). Fmoc-L-valine (3.39 g, 10.0 mmol) and HBTU (3.79 g, 10.0 mmol) were partially dissolved in DMF (10 mL) with stirring. DIEA (1.74 mL, 10.0 mmol) was added, and the solution was allowed to stir for an additional 20 min. The solution was transferred to a flask containing **3** (1.78 g, 5.0 mmol), DMF (5 mL) was added, and the reaction mixture was allowed to stir at room temperature for 22 h. The solvent was evaporated in vacuo, and the residue was partitioned between EtOAc and 1 N $NaHSO_4$. The organic layer was extracted two more times with 1 N $NaHSO_4$, once with brine, three times with saturated $NaHCO_3$, and once with brine. The organic layer was dried with $MgSO_4$ and the solvent was evaporated in vacuo. The residue was purified by silica gel flash column chromatography, eluting with 1% MeOH in CH_2Cl_2. The solvent was removed in vacuo to yield **3a** (3.28 g, 97%) as an off-white foam. ^{1}H NMR (acetone-d_6, 300 MHz) δ 9.26 (s, 1H), 7.85 (d, 2H, J = 7.5 Hz), 7.70 (d, 2H, J = 8.8 Hz), 7.70 (d, 2H, J = ~8 Hz), 7.47 (d, 2H, J = 8.9 Hz), 7.39 (dd, 2H, J = 7.4 Hz, 7.4 Hz), 7.29 (dd, 2H, J = 7.3 Hz, 7.3 Hz), 7.02 (d, 2H, J = 8.8 Hz), 6.95 (d, 2H, J = 8.8 Hz), 6.67 (d, 1H, J = 8.9 Hz), 4.32 (m, 2H), 4.23 (dd, 1H, J = 7.2 Hz, 14.3 Hz), 4.07 (dd, 1H, J = 7.0 Hz, 8.9 Hz), 3.18 (s, 3H), 3.12 (s, 3H), 2.14 (m, 1H), 1.51 (s, 9H), 0.97 (d, 6H, J = 6.8 Hz). HRMS: calcd for $C_{40}H_{44}N_4O_6Na$ $(M+Na)^+$, 699.3158; found, 699.3153.

1-(9‴-Fluorenylmethyloxycarbonyl-L-valyl-(4′-aminophenyl))-3-(4″-carboxyphenyl)-1,3-dimethylurea (4). Compound **3a** (3.19 g, 4.71 mmol) was dissolved in CH_2Cl_2 (20 mL) with stirring, and anisole (2 mL) was added. The reaction mixture was cooled on an ice bath to 0 °C, and TFA (20 mL) was added. The reaction was allowed to stir for 9 h at 0 °C, and then for 1 h at room temperature. The solvent was evaporated in vacuo, and the residue was coevaporated several times with CH_2Cl_2. The residue was partitioned between CH_2Cl_2 and 1 N $NaHSO_4$, and the organic layer was extracted two more times with 1 N $NaHSO_4$. The aqueous layers were combined and extracted three times with CH_2Cl_2. The organic layers were pooled, dried with $MgSO_4$, and the solvent was removed in vacuo to afford **4** (2.85 g, 97%) as an off-white foam. ^{1}H NMR (acetone-d_6, 300 MHz) δ 9.26 (s, 1H), 7.85 (d, 2H, J = 7.5 Hz), 7.77 (d, 2H, J = 8.7 Hz), 7.71 (dd, 2H, J = 6.8 Hz, 6.8 Hz), 7.46 (d, 2H, J = 8.8 Hz), 7.39 (dd, 2H, J = 7.4 Hz, 7.4 Hz), 7.28 (d, 2H, J = 7.6 Hz), 7.05 (d, 2H, J = 8.8 Hz), 6.95 (d, 2H, J = 8.9 Hz), 6.67 (d, 1H, J = 9.0 Hz), 4.32 (m, 2H), 4.23 (dd, 1H, J = 7.0 Hz, 14.1 Hz), 4.07 (dd, 1H, J = 6.9 Hz, 9.0 Hz), 3.19 (s, 3H), 3.14 (s, 3H), 2.12 (m, 1H), 0.96 (d, 6H, J = 6.8 Hz). HRMS: calcd for $C_{36}H_{36}N_4O_6Na$ $(M+Na)^+$, 643.2533; found, 643.2547.

Coupling of 4 to Wang resin to generate resin-bound intermediate 9. Wang resin (0.85 mmol/g substitution level, 1.18 g, 1 mmol), **4** (931 mg, 1.5 mmol), and DMAP (12.2 mg, 0.1 mmol) were dissolved/suspended in 12 mL CH_2Cl_2 with stirring using anhydrous conditions under Ar. To the reaction mixture was added DIPC (266 μL, 1.7 mmol), and the reaction mixture was allowed to stir under Ar for 12 h. The reaction mixture was filtered and the resin washed with CH_2Cl_2 and MeOH, alternating between the two. The resin was dried under vacuum, then a small portion was deprotected with 20% piperidine/DMF and used to determine the level of derivatization using the picric acid assay. The A_{358} of the filtrate indicated a derivatization level of 52%. The total weight of derivatized resin **9** was 1.65 g.

Linear peptide derivative 11. Derivatized Wang resin **9** (1.65 g, equivalent to 1 mmol of original Wang resin) was washed with DMF in a fritted synthesis vessel and then deprotected with 20% piperidine/DMF for 25 min with gentle mixing. The solution was removed via suction and the resin was washed with DMF and CH_2Cl_2, alternating between the two and ending with DMF. A Kaiser ninhydrin test performed on a resin sample was positive. Fmoc-L-Lys(Z)-OH (1.01 g, 2.00 mmol) and HBTU (759 mg, 2 mmol) were partially dissolved in DMF (3 mL) with stirring, and DIEA (523 μL, 3 mmol) was added. After stirring for 15 min, the solution was added to the resin. Additional DMF (1.0 mL) was used to rinse the reaction vessel and was then added to the resin to make a free-flowing slurry. The slurry was mixed gently for 2 h, then the solution was removed via suction. The

resin was washed with DMF, CH_2Cl_2, and finally DMF. A Kaiser test performed on a resin sample was negative. The above procedure was repeated to couple Fmoc-D-Trp-OH (853 mg, 2.00 mmol) and then Fmoc-L-Tyr (2,6-dichlorobenzyl)-OH (1.12 g, 2.00 mmol). In each case the derivatized resin gave a negative Kaiser test. The resin was deprotected with 20% piperidine/DMF, the solution was removed via suction, and the resin was washed with DMF, CH_2Cl_2, DMF, CH_2Cl_2, and air dried. The resin was suspended in triisopropylsilane: anisole:TFA:CH_2Cl_2 (6:4:25:15) (25 mL), and was stirred for 2 h. The resin was filtered and washed with TFA and CH_2Cl_2, and the filtrate was concentrated in vacuo. The residue was co-evaporated several times with CH_2Cl_2, and then triturated with pentane:Et_2O (2:1). The residue was dissolved in THF, concentrated in vacuo, and the residue was coevaporated several times with CH_2Cl_2. The residue was purified by preparative reverse-phase HPLC on a C18 column, using mobile phases of water and CH_3CN containing 0.1% TFA. The eluate was lyophilized, the residue was coevaporated from THF, and the residual solvent was removed in vacuo to afford the TFA salt of **11** (294 mg, 44%) as a tan solid. HRMS: calcd for $C_{62}H_{68}N_9O_{10}Cl_2$ $(M+H)^+$, 1168.4466; found, 1168.4492.

Cyclization of 11 to 11a. Protected linear peptide derivative **11** (134 mg, 104 μmol) and HATU (43.7 mg, 114 μmol) were dissolved in anhydrous DMF (10.4 mL) in an oven-dried flask, and the solid was dissolved with stirring. DIEA (63.7 μL, 365 μmol) was added, and the reaction vessel was purged with Ar. The reaction mixture was allowed to stir for 20 h, the solvent was removed in vacuo, and the residue was partitioned between EtOAc and saturated $NaHCO_3$. The EtOAc layer was extracted two times more with saturated $NaHCO_3$, once with brine, three times with 1 N $NaHSO_4$, and once with brine. The organic layer was dried with $MgSO_4$, the solvent was removed in vacuo, and the residue was coevaporated twice with CH_2Cl_2 to afford the protected cyclic product **11a** (105 mg, 88%) as a yellow-brown solid. HRMS: calcd for $C_{62}H_{65}N_9O_9Cl_2Na$ $(M+Na)^+$, 1172.4180; found, 1172.4196.

Template-constrained cyclic peptide DJS631. Protected cyclic peptide **11a** (40 mg, 34.7 μmol) was dissolved in MeOH (12.5 mL), H_2O (1.5 mL), 88% HCOOH (1.65 mL) with stirring, and the solution was sparged with Ar. To the solution was added 10 wt% Pd/C (55.5 mg, 52.2 μmol Pd, 150 mol% Pd), and the reaction mixture was again sparged with Ar. The reaction mixture was allowed to stir under Ar for 30 h, and the mixture was filtered through Celite. The filter bed was washed with H_2O and MeOH, and the filtrate was concentrated in vacuo. The residue was coevaporated with H_2O/MeOH, several times with MeOH, and then purified by preparative reverse-phase HPLC on a C18 column with mobile phases consisting of water and CH_3CN containing 0.1% TFA. The eluate was lyophilized, the residue was taken up into H_2O, filtered, and lyophilized again to afford the TFA salt of **DJS631** (15.7 mg, 46%) as an off-white solid. HRMS: calcd for $C_{47}H_{55}N_9O_7Na$ $(M+Na)^+$, 880.4122; found, 880.4147.

Ethyl 3-iodobenzoate. 3-Iodobenzoic acid (10.0 g, 40.3 mmol) and DMAP (1.48 g, 12.1 mmol) were dissolved in EtOH (130 mL) with stirring, and the solution was cooled to 0 °C on an ice bath. Dicyclohexylcarbodiimide (DCC) (9.98 g, 48.4 mmol) was added, and the reaction was allowed to stir for 16 h, gradually warming to room temperature. The reaction mixture was filtered, the solid washed with EtOAc, and the filtrate was concentrated in vacuo. The residue was purified by silica gel flash column chromatography, eluting with 3% EtOAc in hexanes. The solvent was removed in vacuo to afford the title compound (10.69 g, 96%) as a yellow oil. ^1H NMR ($CDCl_3$, 300 MHz) δ 8.38 (s, 1H), 8.01 (d, 1H, $J=7.8$ Hz), 7.88 (d, 1H, $J=7.8$ Hz), 7.18 (dd, 1H, $J=7.9$ Hz, 7.9 Hz), 4.38 (q, 2H, $J=7.1$ Hz), 1.40 (t, 3H, $J=7.1$ Hz). HRMS: calcd for $C_9H_9O_2I$ $(M)^+$, 275.9647; found, 275.9643.

3-Ethylcarboxy-2′-formylbiphenyl (5). Ethyl 3-iodobenzoate (5.06 g, 18.3 mmol) was dissolved in toluene (33 mL) with stirring. Aqueous 2 M Na_2CO_3 (16.7 mL) was added, the reaction mixture was purged with Ar, and $Pd(PPh_3)_4$ (578 mg, 0.5 mmol, 3 mol% Pd) was added, repurging the reaction mixture with Ar. 2-Formylbenzeneboronic acid (2.50 g, 16.7 mmol) was dissolved in EtOH (8.3 mL) and added to the reaction mixture, and the reaction mixture was purged with Ar again. The reaction mixture was heated to reflux and allowed to stir for 14 h. The solvent was evaporated from the reaction mixture in vacuo, and the residue was purified by silica gel flash column chromatography, eluting with 5% EtOAc in hexanes. The solvent was removed in vacuo to afford **5** (3.21 g, 76%) as a light yellow oil. ^1H NMR ($CDCl_3$, 300 MHz) δ 9.96 (s, 1H), 8.16–8.04 (m, 3H), 7.68 (dd, 1H, $J=7.5$ Hz, 7.5 Hz), 7.59–7.52 (m, 3H), 7.46 (d, 1H, $J=7.5$ Hz), 4.41 (q, 2H, $J=7.1$ Hz), 1.41 (t, 3H, $J=7.1$ Hz). HRMS: calcd for $C_{16}H_{15}O_3$ $(M+H)^+$, 255.1021; found, 255.1011.

3-Ethylcarboxy-2′-hydroxyiminobiphenyl (6). Compound **5** (3.18 g, 12.5 mmol) was dissolved in THF (30 mL) with stirring, and pyridine (1.52 mL, 18.8 mmol) was added. $HONH_2{\cdot}HCl$ (1.13 g, 16.3 mmol) was added, followed by EtOH (40 mL), and the reaction mixture was allowed to stir for 14 h. The reaction mixture was concentrated in vacuo, and the residue was partitioned between 1 N $NaHSO_4$ and EtOAc. The aqueous layer was extracted three times more with EtOAc, the EtOAc layers were combined, dried with $MgSO_4$, and the solvent evaporated in vacuo. The residue was purified by silica gel flash column chromatography, eluting with 15% EtOAc in hexanes. The eluate was concentrated in vacuo to afford **6** (3.07 g, 91%) as a white solid. ^1H NMR (acetone-d_6, 300 MHz) δ 10.39 (s, 1H), 8.07 (d, 1H, $J=7.2$ Hz), 8.00–7.93 (m, 3H), 7.66–7.58 (m, 2H), 7.52–7.36 (m, 3H), 4.37 (q, 2H, $J=7.1$ Hz), 1.36 (t, 3H, $J=7.1$ Hz). HRMS: calcd for $C_{16}H_{16}NO_3$ $(M+H)^+$, 270.1130; found, 270.1137.

3-Ethylcarboxy-2′-aminomethylbiphenyl, hydrochloride salt (7). Compound **6** (2.98 g, 11.1 mmol) was dissolved with stirring in 1:1 EtOH:HOAc (66 mL) and the solution was cooled to 0 °C on an ice bath. Zn dust (10.85 g,

166.0 mmol) was added to the reaction mixture in small portions over the course of 30 min. The ice bath was removed, and the mixture was allowed to stir for 28 h. The reaction mixture was filtered, and the solid was washed with EtOH. The filtrate was concentrated in vacuo, and the residue was dissolved in EtOAc and saturated Na_2CO_3. The pH of the aqueous layer was adjusted to ~12 with 1 N NaOH, and the layers were shaken together and separated. The aqueous layer was extracted three times more with EtOAc, and the organic layers were combined, dried with $MgSO_4$, and concentrated in vacuo. The residue was dissolved in EtOAc, and anhydrous HCl gas was bubbled through the solution with stirring for 10 min, during which time a solid precipitated. The mixture was cooled to 0 °C on an ice bath, and then filtered. The solid was washed with ice-cold EtOAc, and residual solvent was removed from it under vacuum to afford **7** (2.23 g, 69%) as a white powder. ^{1}H NMR (dimethylsulfoxide-d_6, 300 MHz) δ 8.48 (bs, 3H), 8.01 (d, 1H, J = 7.4 Hz), 7.89 (s, 1H), 7.76–7.61 (m, 3H), 7.54–7.44 (m, 2H), 7.32 (d, 1H, J = 7.2 Hz), 4.33 (q, 2H, J = 7.1 Hz), 3.90 (d, 2H, J = 5.0 Hz), 1.32 (t, 3H, J = 7.1 Hz). HRMS: calcd for $C_{16}H_{18}NO_2$ $(M+H)^+$, 256.1338; found, 256.1350.

3-Carboxy-2-(9″-fluorenylmethyloxycarbonyl-L-valyl-aminomethyl)biphenyl (8). Compound **7** (817 mg, 2.80 mmol) was dissolved in THF (20 mL) with stirring. 10 N NaOH (280 μL) was added, followed by 1 N NaOH (20 mL), and the mixture was heated to reflux. The reaction mixture was stirred at reflux for 8 h. The reaction mixture was allowed to cool, and concentrated HCl (aq) was added to the mixture with stirring until the solution had a pH of 1. The organic solvent was evaporated in vacuo, and the remaining aqueous solution was lyophilized to give solid **7a**. Fmoc-L-Val-OH (1.90 g, 5.60 mmol) and HBTU (2.12 g, 5.60 mmol) were partially dissolved in DMF (6 mL) with stirring, and DIEA (1.46 mL, 8.40 mmol) was added. The solution was allowed to stir for 15 min, and was then added to the lyophilized residue **7a**, which was dissolved with stirring. Additional DMF (3 mL) was added, and the reaction mixture was allowed to stir for 24 h. The solvent was removed in vacuo, and the residue was partitioned between CH_2Cl_2 and 3.7% HCl (aq). The CH_2Cl_2 layer and the solid suspended in it were separated from the aqueous layer, and the aqueous layer was extracted three times more with CH_2Cl_2. The organic layers were pooled and the solvent evaporated in vacuo. The residue was purified by silica gel flash column chromatography, eluting with 1% MeOH/1% HOAc in CH_2Cl_2. The eluate was concentrated in vacuo, coevaporating four times with THF/toluene, three times with CH_2Cl_2, and twice with EtOAc. The residue was triturated with EtOAc, and the solid was filtered and washed with EtOAc. Residual solvent was evaporated from the solid in vacuo to afford **8** (1.00 g, 65%) as an off-white solid foam. ^{1}H NMR (dimethylsulfoxide-d_6, 300 MHz) δ 8.44 (t, 1H, J = 5.1 Hz), 7.94–7.86 (m, 4H), 7.75–7.70 (m, 2H), 7.54–7.18 (m, 11H), 4.31–4.18 (m, 5H), 3.86–3.80 (m, 1H), 1.96–1.89 (m, 1H), 0.82 (dd, 6H, J = 6.3 Hz). HRMS: calcd for $C_{34}H_{32}N_2O_5Na$ $(M+Na)^+$, 571.2209; found, 571.2221.

Coupling of 8 to Wang resin to generate resin-bound intermediate 10. The derivatization reaction was carried out in essentially the same fashion as that for the coupling of **4** to Wang resin to generate **9**. Wang resin (1.00 g, 850 μmol) was derivatized with compound **8** (700 mg, 1.28 mmol) using DIPC (399 μL, 2.55 mmol) and DMAP (20.8 mg, 170 μmol) in CH_2Cl_2 (12 mL) for 48 h. During filtration, the resin was washed with DMF and MeOH rather than CH_2Cl_2 and MeOH. The derivatization level of the resin **10**, measured by the picric acid assay, was 36%, and the total weight of the resin was 1.16 g.

Linear peptide derivative 12. Linear peptide intermediate **12** was derived from resin-bound intermediate **10** in essentially the same fashion as peptide intermediate **11** was derived from resin-bound intermediate **9**. To resin-bound intermediate **10** (1.16 g, equivalent to 850 μmol original Wang resin) were coupled in succession Fmoc-L-Lys(Z)-OH (641 mg, 1.28 mmol), Fmoc-D-Trp-OH (544 mg, 1.28 mmol), and Fmoc-L-Tyr(2,6-dichlorobenzyl)-OH (717 mg, 1.28 mmol), using HBTU (484 mg, 1.28 mmol) and DIEA (370 μL, 2.12 mmol) in DMF (3.5 mL), and coupling times of 2–2.5 h. The peptide was deprotected, cleaved from resin, and purified by preparative reverse-phase HPLC as described for the synthesis of **11**. The eluate was lyophilized, the residue was coevaporated from THF, and the residual solvent was removed in vacuo to afford the TFA salt of **12** (124 mg, 33%) as a tan solid. HRMS: calcd for $C_{60}H_{63}N_7O_9Cl_2Na$ $(M+Na)^+$, 1118.3962; found, 1118.3913.

Cyclization of 12 to 12a. The cyclization of **12** to **12a** was carried out in the same fashion as the cyclization of **11** to **11a**. Peptide derivative **12** (122 mg, 101 μmol) was treated with HATU (42.1 mg, 111 μmol) and DIEA (61.4 μL, 353 μmol) in anhydrous DMF (10.1 mL) for 14 h. The reaction mixture was worked up as described for the cyclization of **11**, to afford **12a** (88 mg, 81%) as a tan solid. HRMS: calcd for $C_{60}H_{61}N_7O_8Cl_2Na$ $(M+Na)^+$, 1100.3848; found, 1100.3865.

Template-constrained cyclic peptide DJS811. The deprotection of **12a** to afford **DJS811** was carried out in the same fashion as the deprotection of **11a** to afford **DJS631**. Protected cyclic peptide **12a** (85 mg, 79 μmol) was treated for 18 h with 88% HCOOH (1 mL) and 10 wt% Pd/C (126 mg, 118 μmol Pd, 150 mol% Pd) in MeOH (10 mL) and H_2O (1 mL) under positive pressure of Ar. The reaction mixture was worked up and purified by preparative reverse-phase HPLC as described for the deprotection of **11a** to afford the TFA salt of **DJS811** (35.4 mg, 50%) as a white solid. HRMS: calcd for $C_{45}H_{51}N_7O_6Na$ $(M+Na)^+$, 808.3798; found, 808.3807.

Radioligand binding

Receptor binding assays on cloned somatostatin receptors were performed using human SSTR1, mouse SSTR2B, mouse SSTR3, human SSTR4, and both rat and human SSTR5 expressed in mammalian cells. Cells were harvested, membranes were prepared, binding of **DJS631** and **DJS811** was assayed, and IC_{50}s were calculated essentially as described.[64] (3-[^{125}I]*iodotyrosyl*^{11})

Somatostatin-14(tyr^{11}), obtained from Amersham, was used as the receptor labeling agent.

Matrigel angiogenesis animal model

Matrigel is an extract from murine tumor containing laminin, collagen IV, heparin sulfate, and proteoglycans. When the extract is supplemented with growth factors and injected subcutaneously into mice, an intense angiogenic response can be observed. This model has been used to study the stimulation of angiogenesis by a variety of factors.[51,65,66]

Animals

Animal studies were conducted in a facility fully accredited by the American Association for the Accreditation of Laboratory Animal Care. Female C57BI/6 mice, 6–8 weeks old (Charles River Laboratory) were housed 10 per cage in a room controlled to 20±2 °C and 50±10% relative humidity, with a 12 h light/dark cycle. The animals were fed a standard pelleted mouse chow (Agway), and water was available ad libitum.

Mini-pump implantation

Mini-pumps were purchased from Alza (#2002). The pumps were filled 3 h prior to implantation and incubated in ~5 mL of phosphate-buffered saline (PBS) at 37 °C to allow the flow to start. Animals were anesthetized with 25 mg/kg ketamine and 5 mg/kg Rompun mix, and a small 2 cm incision was made on the dorsal skin near the scapula of the mouse. Using forceps, a 1 inch tunnel was made subcutaneously, into which the pump was inserted; the wound was closed with a clip.

Matrigel preparation and use

Matrigel (Collaborative Biomedical) was allowed to thaw overnight on ice at 4 °C, and aliquots of the thawed gel were placed into cold polypropylene tubes. For both the positive control and treated animals, bFGF (Gibco) was added to the gel (500 ng/mL); no bFGF was added to the negative control gel aliquots. Protein tyrosine kinase inhibitors were dissolved in dimethylsulfoxide and added directly to the gel aliquots. The tubes were capped and rotated end over end at 4 °C for at least 3 h. Gel aliquots (0.5 mL) were injected subcutaneously into the ventral midline of the mice; the liquid gel hardened once inside the animal. After 7 days, the mice were sacrificed, and the gel with the attached peritoneal lining was removed by dissecting away the skin from the gel. The gel samples were then assayed for angiogenesis, using a hemoglobin and an immunohistochemical assay.

Hemoglobin assay

Gel samples were transferred into microfuge tubes containing 0.5 mL of a cell lysis reagent (Sigma #R1129) and crushed with a pestle. They were allowed to sit overnight at 4 °C and were then spun in a microfuge. Aliquots of the lysate (200 μL) were added to 1.3 mL of Drabkin reagent solution (Hgb kit, Sigma #525A). The absorbance at 540 nm of the resulting colored mixture was read on a spectrophotometer (the absorbance intensity at this wavelength is proportional to total hemoglobin content). Hemoglobin concentration was calculated from a five-point standard curve. Hemoglobin data is presented as grams of hemoglobin/dL and as percent inhibition of angiogenesis: % inhibition = 100[1−(treated−negative control)/(positive control−negative control)].

Immunohistochemistry and visualization

Matrigel with attached peritoneal lining was placed in cold M−1 embedding matrix (Lipshaw) and snap frozen in 2-methylbutane chilled on dry ice. Thin sections, 10 μm thick, were placed on (poly-L-lysine)-coated slides (Polyscience), air dried and stored in a dessicated container at −80 °C. Immediately before use, the slides were air dried at room temperature, placed in MeOH:3% H_2O_2 (4:1) for 20 min, and then rinsed in 0.05 M Tris–HCl (pH 7.4) (Tris = tris(hydroxymethyl)aminomethane) buffer. Tissue was digested with 0.05% Pronase (Calbiochem) and 0.11% ethylenediaminetetraacetic acid (EDTA) in PBS for 20 min at 37 °C, then rinsed twice in Tris buffer. Next, tissue samples were fixed in 4 °C acetone for 8 min and rinsed three times in Tris buffer. Rat anti-mouse monoclonal CD31 (PECAM PharMingen #01951D) or as a control IgG_{2a}, *k* isotype standard (PharMingen #11021D) was applied at 5 μg/mL, and the slides were incubated overnight at room temperature. Slides were rinsed twice in Tris buffer, and biotin-labeled goat anti-rat IgG (H + L, 5 μg/mL, Southern Biotechnology #3050-08) was applied. The slides were incubated at room temperature for 40 min, and were then rinsed three times in Tris buffer. Streptavidin-alkaline phospatase conjugate (10–20 units/mL, Boehringer-Mannheim #1089161) was applied for 40 min at room temperature, and the slides were rinsed three times in Tris buffer. HistoMark Red (Kirkegaard & Perry Laboratories #55-69-00) was used to visualize the alkaline-phosphatase-labeled antigens. The endothelial cell content of the Matrigel was observed using the Optomax image analysis system at 20× magnification. Fields were selected in a consistent pattern using the peritoneal lining for orientation.

Acknowledgements

This work was supported by grant CHE-34646 to William F. DeGrado. D. J. S. was supported in part by the DuPont Merck Pharmaceutical Co. postdoctoral fellows program.

References and Notes

1. Rose, G. D.; Gierasch, L. M.; SmithJ. A. *Advances in Protein Chemistry*; Academic Press: New York, 1985; pp 1–109.
2. Kyle, D. J.; Blake, P. R.; Smithwick, D.; Green, L. M.; Martin, J. A.; Sinsko, J. A.; Summers, M. F. *J. Med. Chem.* **1993**, *36*, 1450.

3. Nikiforovich, G. V.; Marshall, G. R. *Int. J. Pept. Protein Res.* **1993**, *42*, 181.
4. Garcia, K. C.; Ronco, P. M.; Verroust, P. J.; Brünger, A. T.; Amzel, L. M. *Science* **1992**, *257*, 502.
5. Rini, J. M.; Schulze-Gahmen, U.; Wilson, I. A. *Science* **1992**, *255*, 959.
6. Stanfield, R. L.; Fieser, T. M.; Lerner, R. A.; Wilson, I. A. *Science* **1990**, *248*, 712.
7. Dyson, H. J.; Cross, K. J.; Houghten, R. A.; Wilson, I. A.; Wright, P. E.; Lerner, R. A. *Nature* **1985**, *318*, 480.
8. Imperiali, B.; Spencer, J. R.; Struthers, M. D. *J. Am. Chem. Soc.* **1994**, *116*, 8424.
9. Haubner, R.; Finsinger, D.; Kessler, H. *Angew. Chem., Int. Ed. Engl.* **1997**, *36*, 1374.
10. Bach, A. C., II; Eyermann, C. J.; Gross, J. D.; Bower, M. J.; Harlow, R. L.; Weber, P. C.; DeGrado, W. F. *J. Am. Chem. Soc.* **1994**, *116*, 3207.
11. Haubner, R.; Schmitt, W.; Hölzemann, G.; Goodman, S. L.; Jonczyk, A.; Kessler, H. *J. Am. Chem. Soc.* **1996**, *118*, 7881.
12. Etzkorn, F. A.; Guo, T.; Lipton, M. A.; Goldberg, S. D.; Bartlett, P. A. *J. Am. Chem. Soc.* **1994**, *116*, 10412.
13. Matter, H.; Kessler, H. *J. Am. Chem. Soc.* **1995**, *117*, 3347.
14. Kline, A. D.; Braun, W.; Wüthrich, K. *J. Mol. Biol.* **1986**, *189*, 377.
15. Pflugrath, J. W.; Wiegand, G.; Huber, R. *J. Mol. Biol.* **1986**, *189*, 383.
16. Wang, J.; Yan, Y.; Garrett, T. P. J.; Liu, J.; Rodgers, D. W.; Garlick, R. L.; Tarr, G. E.; Husain, Y.; Reinherz, E. L.; Harrison, S. C. *Nature* **1990**, *348*, 411.
17. Ryu, S.-E.; Kwong, P. D.; Truneh, A.; Porter, T. G.; Arthos, J.; Rosenberg, M.; Dai, X.; Xuong, N.-H.; Axel, R.; Sweet, R. W.; Hendrickson, W. A. *Nature* **1990**, *348*, 419.
18. Chen, S.; Chrusciel, R. A.; Nakanishi, H.; Raktabutr, A.; Johnson, M. E.; Sato, A.; Weiner, D.; Hoxie, J.; Saragovi, H. U.; Greene, M. I.; Kahn, M. *Proc. Natl. Acad. Sci. USA* **1992**, *89*, 5872.
19. Schneider, J. P.; Kelly, J. W. *Chem. Rev.* **1995**, *95*, 2169.
20. Gillespie, P.; Cicariello, J.; Olson, G. L. *Biopolymers* **1997**, *43*, 191.
21. Kitagawa, O.; Vander Velde, D.; Dutta, D.; Morton, M.; Takusagawa, F.; Aubé, J. *J. Am. Chem. Soc.* **1995**, *117*, 5169.
22. Ernest, I.; Kalvoda, J.; Rihs, G.; Mutter, M. *Tetrahedron Lett.* **1990**, *31*, 4011.
23. Sarabu, R.; Lovey, K.; Madison, V. S.; Fry, D. C.; Greeley, D. N.; Cook, C. M.; Olson, G. L. *Tetrahedron* **1993**, *49*, 3629.
24. Boger, D. L.; Myers, J. B., Jr. *J. Org. Chem.* **1991**, *56*, 5385.
25. Elseviers, M.; van der Auwera, L.; Pepermans, H.; Tourwé, D.; van Binst, G. *Biochem. Biophys. Res. Commun.* **1988**, *154*, 515.
26. Pavone, V.; Lombardi, A.; Saviano, M.; Di Blasio, B.; Nastri, F.; Fattorusso, R.; Maglio, O.; Isernia, C. *Biopolymers* **1994**, *34*, 1505.
27. Pavone, V.; Lombardi, A.; Nastri, F.; Saviano, M.; Maglio, O.; D'Auria, G.; Quartara, L.; Maggi, C. A.; Pedone, C. *J. Chem. Soc., Perkin Trans. 2* **1995**, *5*, 987.
28. Kemp, D. S.; Li, Z. Q. *Tetrahedron Lett.* **1995**, *36*, 4175.
29. Bach, A. C., II; Markwalder, J. A.; Ripka, W. C. *Int. J. Pept. Protein Res.* **1991**, *38*, 314.
30. Nagai, U.; Sato, K.; Nakamura, R.; Kato, R. *Tetrahedron* **1993**, *49*, 3577.
31. Ripka, W. C.; De Lucca, G. V.; Bach, A. C., II; Pottorf, R. S.; Blaney, J. M. *Tetrahedron* **1993**, *49*, 3609.
32. Smythe, M. L.; von Itzstein, M. *J. Am. Chem. Soc.* **1994**, *116*, 2725.
33. Jackson, S.; DeGrado, W.; Dwivedi, A.; Parthasarathy, A.; Higley, A.; Krywko, J.; Rockwell, A.; Markwalder, J.; Wells, G.; Wexler, R.; Mousa, S.; Harlow, R. *J. Am. Chem. Soc.* **1994**, *116*, 3220.
34. Brazeau, P.; Vale, W.; Burgus, R.; Ling, N.; Butcher, M.; Rivier, J.; Guillemin, R. *Science* **1973**, *179*, 77.
35. Arison, B. H.; Hirschmann, R.; Veber, D. F. *Bioorg. Chem.* **1978**, *7*, 447.
36. Reisine, T.; Bell, G. I. *Endocr. Rev.* **1995**, *16*, 427.
37. Veber, D. F.; Saperstein, R.; Nutt, R. F.; Freidinger, R. M.; Brady, S. F.; Curley, P.; Perlow, D. S.; Paleveda, W. J.; Colton, C. D.; Zacchei, A. G.; Tocco, D. J.; Hoff, D. R.; Vandlen, R. L.; Gerich, J. E.; Hall, L.; Mandarino, L.; Cordes, E. H.; Anderson, P. S.; Hirschmann, R. *Life Sci.* **1984**, *34*, 1371.
38. Lamberts, S. W. J.; Krenning, E. P.; Reubi, J.-C. *Endocr. Rev.* **1991**, *12*, 450.
39. Bass, R. T.; Buckwalter, B. L.; Patel, B. P.; Pausch, M. H.; Price, L. A.; Strnad, J.; Hadcock, J. R. *Mol. Pharmacol.* **1996**, *50*, 709.
40. Hocart, S. J.; Jain, R.; Murphy, W. A.; Taylor, J. E.; Morgan, B.; Coy, D. H. *J. Med. Chem.* **1998**, *41*, 1146.
41. Smith, L. E. H.; Kopchick, J. J.; Chen, W.; Knapp, J.; Kinose, F.; Daley, D.; Foley, E.; Smith, R. G.; Schaeffer, J. M. *Science* **1997**, *276*, 1706.
42. Woltering, E. A.; Watson, J. C.; Alperin-Lea, R. C.; Sharma, C.; Keenan, E.; Kurozawa, D.; Barrie, R. *Invest. New Drugs* **1997**, *15*, 77.
43. Folkman, J. *Nature Med.* **1995**, *1*, 27.
44. Souers, A. J.; Virgilio, A. A.; Rosenquist, Å.; Feniuk, W.; Ellman, J. A. *J. Am. Chem. Soc.* **1999**, *121*, 1817.
45. Ankersen, M.; Crider, M.; Liu, S.; Ho, B.; Andersen, H. S.; Stidsen, C. *J. Am. Chem. Soc.* **1998**, *120*, 1368.
46. Rohrer, S. P.; Birzin, E. T.; Mosley, R. T.; Berk, S. C.; Hutchins, S. M.; Shen, D.-M.; Xiong, Y.; Hayes, E. C.; Parmar, R. M.; Foor, F.; Mitra, S. W.; Degrado, S. J.; Shu, M.; Klopp, J. M.; Cai, S.-J.; Blake, A.; Chan, W. W. S.; Pasternak, A.; Yang, L.; Patchett, A. A.; Smith, R. G.; Chapman, K. T.; Schaeffer, J. M. *Science* **1998**, *282*, 737.
47. Yang, L.; Berk, S. C.; Rohrer, S. P.; Mosley, R. T.; Guo, L.; Underwood, D. J.; Arison, B. H.; Birzin, E. T.; Hayes, E. C.; Mitra, S. W.; Parmar, R. M.; Cheng, K.; Wu, T.-J.; Butler, B. S.; Foor, F.; Pasternak, A.; Pan, Y.; Silva, M.; Freidinger, R. M.; Smith, R. G.; Chapman, K.; Schaeffer, J. M.; Patchett, A. A. *Proc. Natl. Acad. Sci. USA* **1998**, *95*, 10836.
48. Yang, L.; Guo, L.; Pasternak, A.; Mosley, R.; Rohrer, S.; Birzin, E.; Foor, F.; Cheng, K.; Shaeffer, J.; Patchett, A. A. *J. Med. Chem.* **1998**, *41*, 2175.
49. Yamaguchi, K.; Matsumura, G.; Kagechika, H.; Azumaya, I.; Ito, Y.; Itai, A.; Shudo, K. *J. Am. Chem. Soc.* **1991**, *113*, 5474.
50. Vanetti, M.; Vogt, G.; Höllt, V. *FEBS* **1993**, *331*, 260.
51. Passaniti, A.; Taylor, R. M.; Pili, R.; Guo, Y.; Long, P. V.; Haney, J. A.; Pauly, R. R.; Grant, D. S.; Martin, G. R. *Lab. Invest.* **1992**, *67*, 519.
52. Coy, D. H.; Rossowski, W. J. *Ciba Found. Symp.* **1995**, *190*, 240.
53. Buscail, L.; Estève, J.-P.; Saint-Laurent, N.; Bertrand, V.; Reisine, T.; O'Carroll, A.-M.; Bell, G. I.; Schally, A. V.; Vaysse, N.; Susini, C. *Proc. Natl. Acad. Sci. USA* **1995**, *92*, 1580.
54. Buscail, L.; Delesque, N.; Estève, J.-P.; Saint-Laurent, N.; Prats, H.; Clerc, P.; Robberecht, P.; Bell, G. I.; Liebow, C.; Schally, A. V.; Vaysse, N.; Susini, C. *Proc. Natl. Acad. Sci. USA* **1994**, *91*, 2315.
55. Lauder, H.; Sellers, L. A.; Fan, T.-P. D.; Feniuk, W.; Humphrey, P. P. A. *Brit. J. Pharm.* **1997**, *122*, 663.
56. Alderton, F.; Lauder, H.; Feniuk, W.; Fan, T.-P. D.; Humphrey, P. P. A. *Brit. J. Pharm.* **1998**, *124*, 323.

57. Hanahan, D. *Science* **1997**, *277*, 48.
58. Maisonpierre, P. C.; Suri, C.; Jones, P. F.; Bartunkova, S.; Wiegand, S. J.; Radziejewski, C.; Compton, D.; McClain, J.; Aldrich, T. H.; Papadopoulos, N.; Daly, T. J.; Davis, S.; Sato, T. N.; Yancopoulos, G. D. *Science* **1997**, *277*, 55.
59. Brecx, V.; Misicka, A.; Verheyden, P.; Tourwé, D.; van Binst, G. *Lett. Pept. Sci.* **1995**, *2*, 165.
60. Haque, T. S.; Gellman, S. H. *J. Am. Chem. Soc.* **1997**, *119*, 2303.
61. de Alba, E.; Jiménez, M. A.; Rico, M. *J. Am. Chem. Soc.* **1997**, *119*, 175.
62. Pearson, D. A.; Lister-James, J.; McBride, W. J.; Wilson, D. M.; Martel, L. J.; Civitello, E. R.; Taylor, J. E.; Moyer, B. R.; Dean, R. T. *J. Med. Chem.* **1996**, *39*, 1361.
63. Stolz, B.; Smith-Jones, P.; Albert, R.; Tolcsvai, L.; Briner, U.; Ruser, G.; Mäcke, H.; Weckbecker, G.; Bruns, C. *Digestion* **1996**, *57*, 17.
64. Liapakis, G.; Fitzpatrick, D.; Hoeger, C.; Rivier, J.; Vandlen, R.; Reisine, T. *J. Biol. Chem.* **1996**, *271*, 20331.
65. Grant, D. S.; Morales, D.; Cid, M. C.; Kleinman, H. K. *Angiogenesis: Molecular Biology, Clinical Aspects*; Plenum Press: New York, 1994; pp 51–60.
66. Kibbey, M. C.; Grant, D. S.; Kleinman, H. K. *J. Natl. Cancer Inst.* **1992**, *84*, 1633.